Supplementary Information for

Gas-induced modulation of carbon nitride morphology in a green one-step calcination strategy

Jie Wu[1], Zheng Liu[1], Mengjie Li, Jinjuan Zhao, Shuwen Li* and Honglei Yang*

State Key Laboratory of Applied Organic Chemistry, Gansu Provincial Engineering Laboratory for Chemical Catalysis, College of Chemistry and Chemical Engineering, Lanzhou University, Lanzhou, 730000, P. R. China

[1]These authors contributed equally to this work.

*Corresponding author.

E-mail addresses: lishw@lzu.edu.cn (Shuwen Li), yanghl@lzu.edu.cn (Honglei Yang)

Text S1. Sample characterization instruments

SEM images were obtained with a Hitachi S-4800 instrument. Transmission electron microscopy (TEM), high-resolution transmission electron microscopy (HRTEM) and EDS mappings were performed on the FEI talos F200s electron microscope. Powder X-ray diffraction (XRD) patterns were carried out on a Rigaku D/max-2400 diffractometer with Cu-Kα radiation. The nitrogen adsorption-desorption isotherms and pore size distribution curves were recorded with an ASAP 2460 analyzer after degassing in a vacuum at 200 °C for 12 h and the SSA was calculated using the Brunauer-Emmett-Teller (BET) method. X-ray photoelectron spectroscopy (XPS) was conducted on an Axis Supra X-ray photoelectron spectrometer with a monochromatic Al Kα X-ray source. Elemental analysis was conducted with a Vario EL cube element analyzer. The content of C and N elements was measured by means of a vario EL cube elemental analyser from Elementar, Germany. Photoluminescence (PL) spectra were acquired using an FLS 920 fluorescence spectrofluorometer. Solid-state UV-vis diffuse reflectance spectra (UV-vis DRS) were operated on a UV-2600 spectrophotometer using $BaSO_4$ as a background. Electron paramagnetic resonance (EPR) spectra were recorded on an ER200DSRC10/12 spectrometer using DMPO as the capture agent.

Text S2. Photoelectrochemical (PEC) measurements

The transient photocurrent response curves, electrochemical impedance spectroscopy (EIS) and Mott-Schottky (M-S) plots were acquired with a CHI 760E

electrochemical workstation (Chenhua Instrument Co., Ltd, China) with a three-electrode configuration (an FTO spin-coated with catalyst, an Ag/AgCl electrode and a Pt slice were employed as the working electrode, reference electrode and counter electrode, respectively). The light source was a 300 W xenon lamp (PLS-SXE300+) with an ultraviolet filter ($\lambda > 420$ nm) at an intensity of 1000 mW cm^{-2}, which was measured with an FZ-A radiometer. The electrolyte was 0.2 M Na_2SO_4 aqueous solution.

FTO spin-coated with catalyst was prepared as follows: 20 mg of photocatalyst was dispersed in 4 mL of solution (1.8 mL of deionized water, 1.8 mL of ethanol and 0.4 mL of Nafion solution). After homogenization by ultrasound, 100 μL of catalyst dispersion was spun on FTO conductive glass. This was repeated five times and the glass was dried at room temperature for photochemical testing. Spin coating parameters: rotation speed 3000 rpm, spin coating time 20 s.

Text S3. Activity of photocatalytic Cr(VI) reduction

The reaction of photo-reduced Cr (VI) following pseudo-first-order kinetic model Eq. (S1)

$$\ln(C_0/C_t) = kt \tag{S1}$$

Where C_0 and C_t represent the concentration at time of 0 and t min, k is the kinetic constant of Cr (VI) reaction, t represents the irradiation time.

The internal quantum efficiency (IQE) is calculated as in Eq. (S2)[1].

$$\mathrm{IQE}(\lambda) = \frac{|j_{ph}| \times 1239.8}{P_{mono} \times \lambda \times (1 - 10^{-A})} \tag{S2}$$

Where λ is the wavelength of monochromatic light (nm), j_{ph} is the optical current density measured by the chronocurrent method (mA cm^{-2}), P_{mono} is the optical power density of monochromatic light calculated from Eq. S3 (mW cm^{-2}), and A is the UV-vis DRS absorbance of the catalyst sample.

$$P_{mono} = 0.1\ P/S \tag{S3}$$

Where P is the optical power of monochromatic light (W), S is the detector light area of 3.14×10^{-4} m^2.

Text S4. Tauc plot to calculate the band gap E_g

$$(Ah\nu)^{1/n} = B(h\nu-E_g) \tag{S4}$$

Where A is the absorbance, h is Planck's constant, ν is the frequency, B is a constant, E_g is the semiconductor forbidden bandwidth, the index n is directly related to the type of semiconductor, the direct bandgap n = 1/2, the indirect bandgap n = 2. Because the carbon nitride is an indirect bandgap semiconductor, therefore, n is taken to be 2. It can be seen from this formula, $(Ah\nu)^{1/n}$ is linearly related to h ν, and therefore, respectively, with $(Ah\nu)^{1/2}$ as the y-axis. hν is plotted as the x-axis, and then the tangent line of the curve is extended in reverse to intersect with the x-axis, hν for the x-axis graph, and then extend the curve tangent to the x-axis intersection, the intersection point hν that is the semiconductor material for the optical indirect band gap E_g.

$$E_{NEH} = E_{Ag/AgCl} + 0.1976\ V \tag{S5}$$

$E_{NHE}$is the potential with the standard hydrogen electrode (NHE) as reference;

$E_{Ag/AgCl}$ is the potential with the Ag/AgCl electrode as reference.

$$E_{VB} = E_{CB} + E_g \tag{S6}$$

E_{VB} is the valence band potential; E_{CB} is the conduction band potential; E_g is the band gap.

Results and Discussion

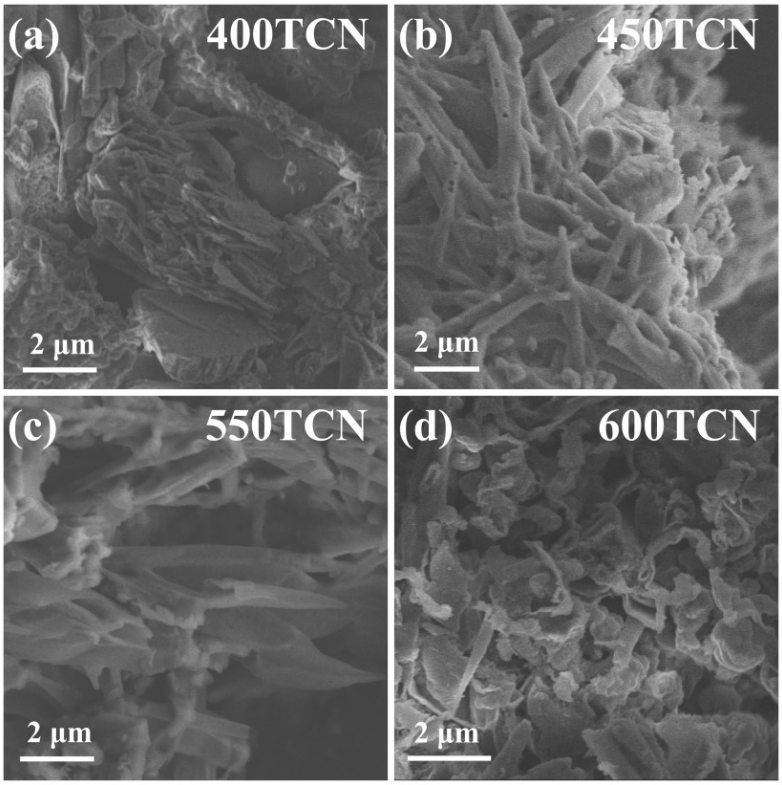

Figure S1. SEM of 400TCN (a), 450TCN (b), 550TCN (c), 600TCN (d).

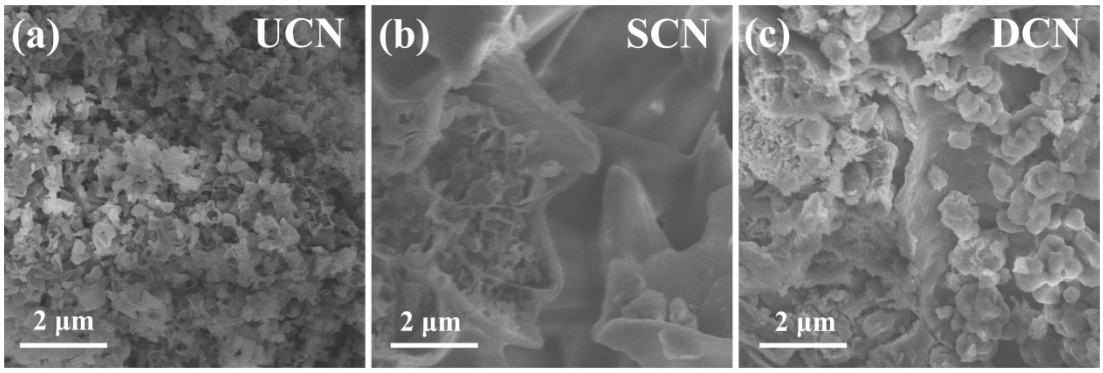

Figure S2. SEM of UCN (a), SCN (b), DCN (c).

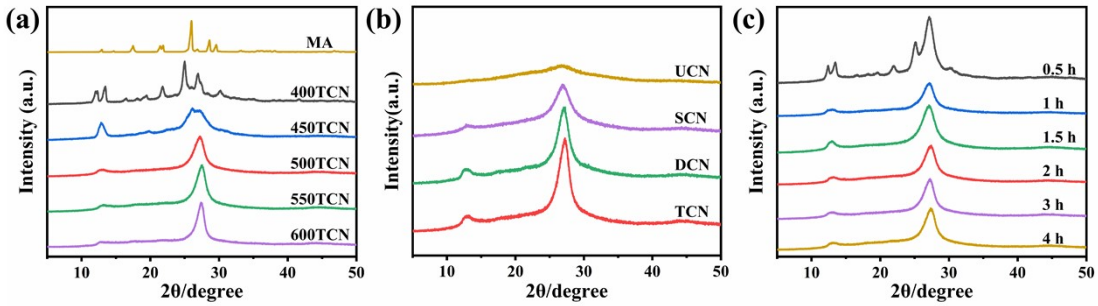

Figure S3. XRD of samples with different calcination temperatures (a), precursors (b), and holding times (c).

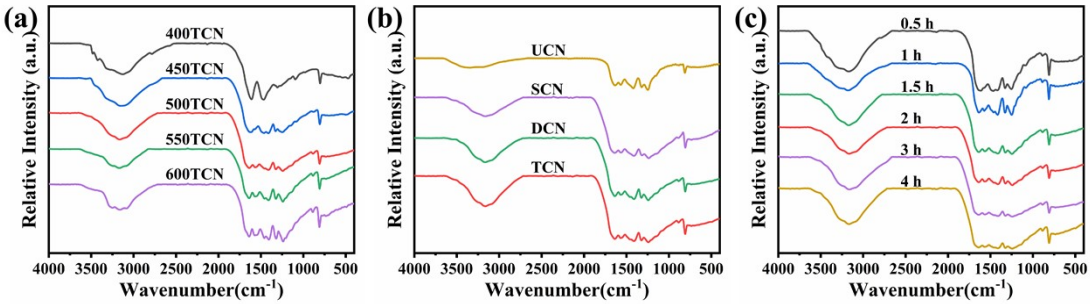

Figure S4. FTIR of samples with different calcination temperatures (a), precursors (b), and holding times (c).

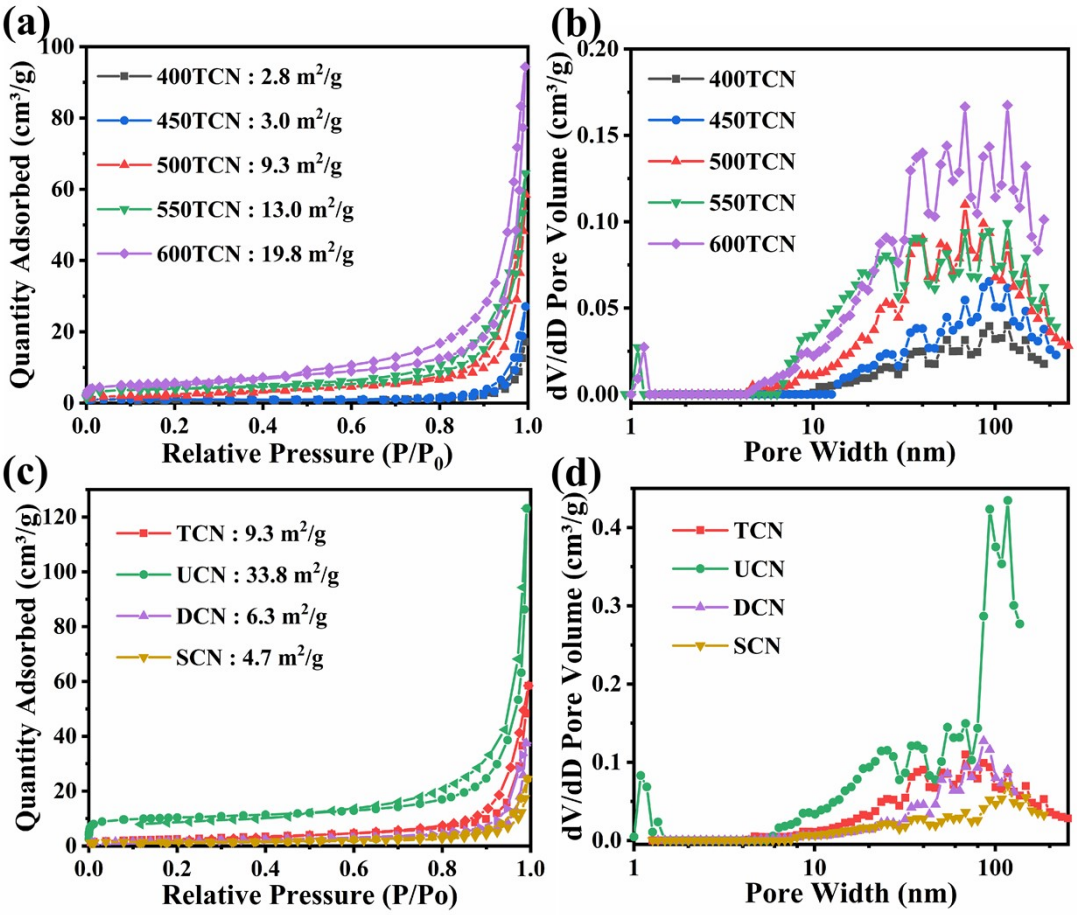

Figure S5. N_2 adsorption-desorption isotherms (a) and pore size distribution (b) for samples with different calcination temperatures; N_2 adsorption-desorption isotherms (c) and pore size distribution (d) for samples with different precursors.

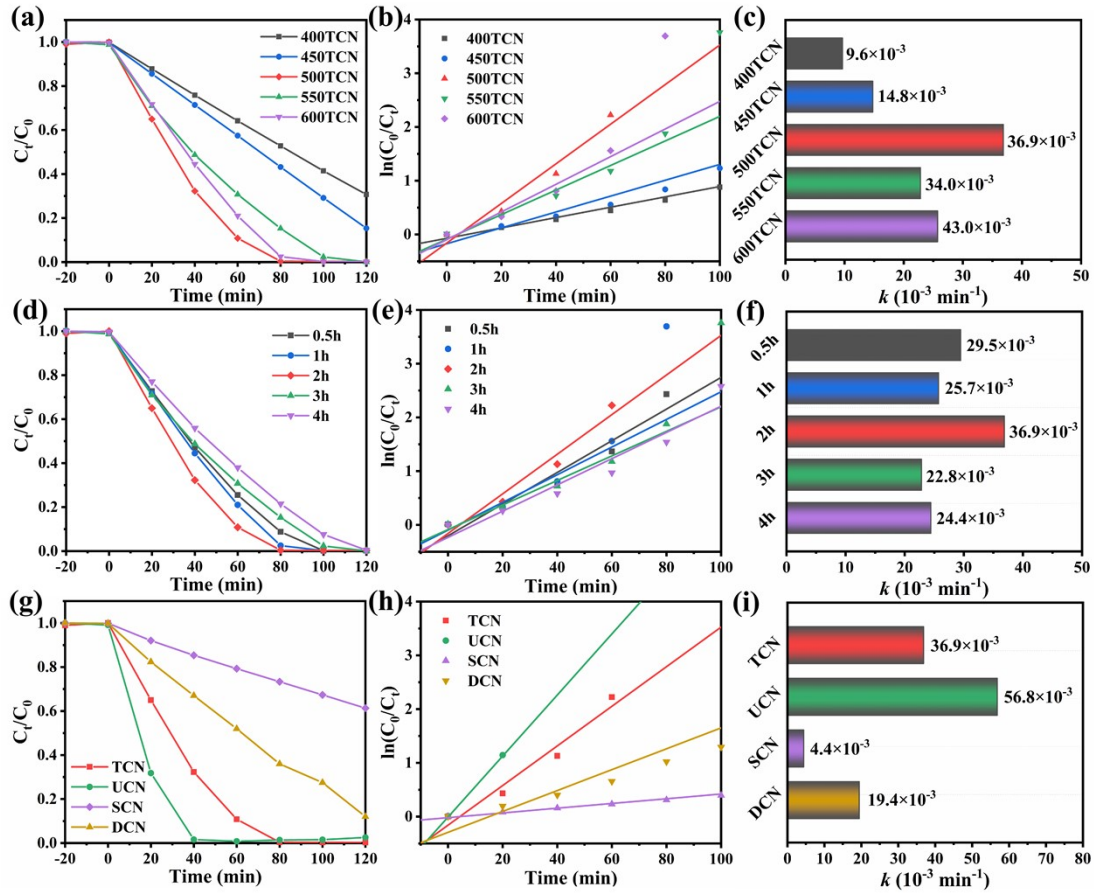

Figure S6. Photocatalytic activity of samples with different calcination temperatures (a), first-order reaction (b), reaction rate constant *k* (c); photocatalytic activity of samples with different holding times (d), first-order reaction (e), reaction rate constant *k* (f); photocatalytic activity of samples with different precursor calcination (g), first-order reaction (h), reaction rate constant *k* (i).

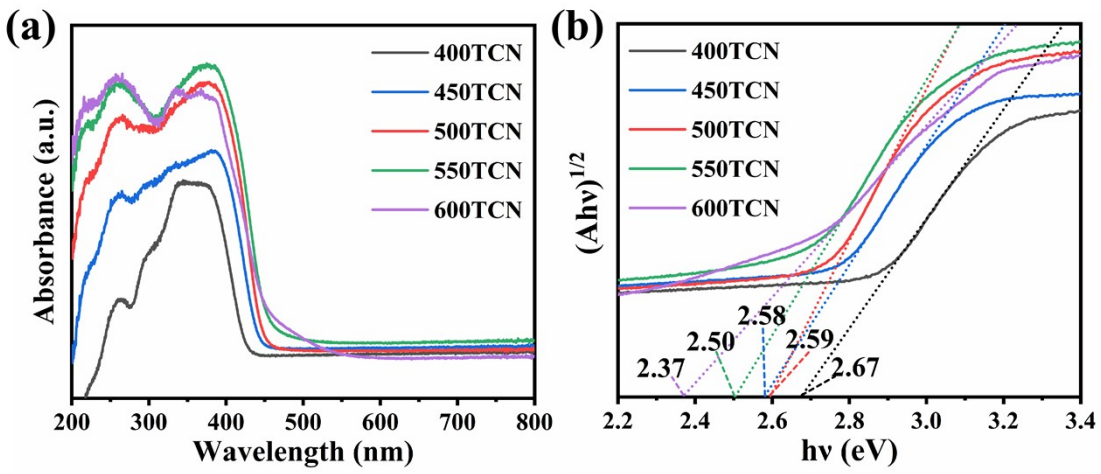

Figure S7. UV-vis DRS (a) and Tauc plot (b) for samples with different calcination temperatures.

Table S1. Nomenclature of carbon nitride samples

Name	Precursor	Heating rate	Calcination temperature	Holding time
TCN-1	Melamine	1 °C min^{-1}	500 °C	2 h
TCN-2.5	-	2.5 °C min^{-1}	-	-
TCN-5	-	5 °C min^{-1}	-	-
TCN-8	-	8 °C min^{-1}	-	-
TCN-10	-	10 °C min^{-1}	-	-
400TCN	Melamine	5 °C min^{-1}	400 °C	2 h
450TCN	-	-	450 °C	
550TCN	-	-	550 °C	
600TCN	-	-	600 °C	
UCN	Urea	5 °C min^{-1}	500 °C	2 h
SCN	Thiourea	-	-	-
DCN	Dicyandiamide	-	-	-

"-" indicates the same as in the previous line.

Table S2. Comparison of tubular carbon nitride

Sample	Precursor	Method	Size	Morphology
TCN-5[This work]	melamine	Calcination (500 °C, 5 °C min^{-1}, 4h)	Conical L: 5-10 μm D: 0.2-0.5 μm	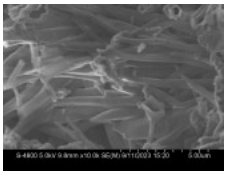
TGCN-B2[2]	cyanuric acid + H_3BO_3 (A), melamine (B)	1. Solutions A and B, mixing, stirring (120 °C, 12h) 2. Calcination	D: 0.5-1 μm	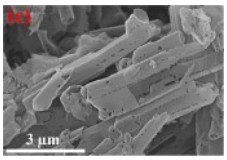
GCNT[3]	isonicotinic acid, melamine	1. Hydrothermal 2. Calcination	Hexagonal D: ~1.5 μm	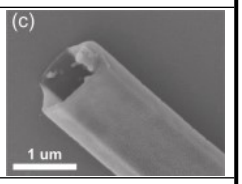
HTCN[4]	melamine	1. Hydrothermal 2. Calcination on N_2 3. Calcination on H_2	Irregular micron	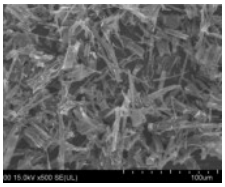
CNA[5]	5-aminouracil, cyanuric acid, melamine	1. Stirring (12h), drying 2. Calcination	D: 0.2-0.4 μm	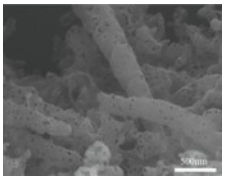
Py-CNT[6]	L-cysteine, urea	1. Grinding and mixing 2. Calcination	D: ~0.13 μm	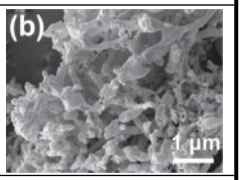
TCN-1.5[7]	urea, melamine	1. Hydrothermal 2. Calcination	Irregular micron	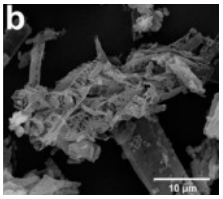
SCN600[8]	trithiocyanuric acid, melamine	1. Ultrasonic, stirring (12h), drying 2. Calcination	D: 0.2-0.5 μm	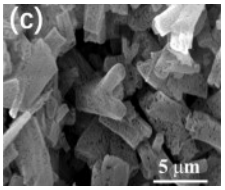
K-CN-2[9]	melamine	1. Hydrothermal with KBr 2. Calcination	L: 15-30 μm D: 2-3 μm	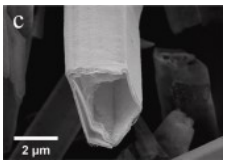

ND-TCN-10[10]	melamine	1. Hydrothermal 2. Calcination with KOH	L: 20-50 μm D: 2-5 μm	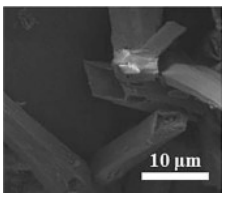
PCN[11]	melamine	1. +SiO_2, mixed, Calcination (600 °C, 4 °C min^{-1}, 4h) 2. HF to remove SiO_2	D: 0.2-0.4 μm	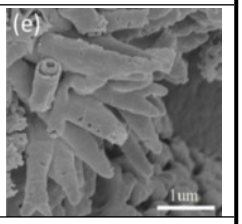
SCN[12]	melamine	1. Calcination→BCN 2. BCN + H_2SO_4, stirring, washing, drying 3. Recalcination	L: 2-4 μm D: 0.5-1 μm	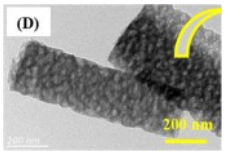
OCN-Tube[13]	melamine	1. Calcination 2. Take the sample from the end wall of the quartz tube	Convoluted Nanosheets D: ~0.02 μm	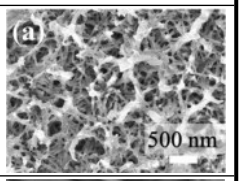
tubular g-C_3N_4[14]	melamine	1. + ethylene glycol + HO_3, stirring, washing, drying 2. Calcination	L: ~20 μm D: ~0.8 μm	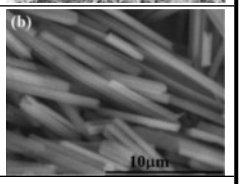
tube-like g-C_3N_4[15]	melamine	1. Shaking in the vibrator to reach a certain pile density 2. Calcination	D: ~0.05 μm	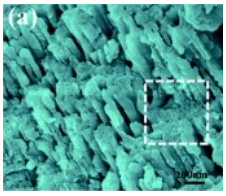

Table S3. Ratio of XPS fitted peak areas for different samples

		N=C-N	C-NH_X	C-C	NH_X	N-$(C)_3$	C=N-C
TCN-1	peak position/eV	288.23	286.15	284.80	401.21	399.84	398.62
	area ratio	80.0%	3.4%	16.6%	8.1%	20.4%	71.5%
TCN-5	peak position/eV	288.32	286.29	284.80	401.42	400.32	398.72
	area ratio	80.5%	2.8%	16.7%	4.3%	21.3%	74.4%
TCN-10	peak position/eV	288.29	286.29	284.80	401.46	400.53	398.68
	area ratio	82.8%	2.0%	15.2%	3.3%	12.8%	83.9%

Table S4. Comparison of photocatalytic reduction activity of Cr(VI) by different g-C_3N_4-based materials

Sample	Catalyst amount	Cr(VI) solution amount	Degradation rate	Reaction rate constant k /min^{-1}
TCN-5[This work]	20 mg	50 mL (100 mg L^{-1})	99.7% (80 min)	0.0369
11CN[16]	50 mg	50 mL (10 mg L^{-1})	90% (40min)	0.0272
CN-PG-S0.5wt.%[17]	50 mg	50 mL (10 mg L^{-1})	99.1% (75 min)	0.0329
B-CN@BS-10[18]	25mg	50 mL (20 mg L^{-1})	86.77 % (150 min)	-
PHCN-1[19]	10 mg	10 mL (30 mg L^{-1})	-	0.033
CN-Br20[20]	50 mg	50 mL (20 mg L^{-1})	61.6% (120 min)	-
OCNv-U_{40}[21]	60 mg	100 mL (50 mg L^{-1})	90.8% (120 min)	-
GCNX[22]	20 mg	40 mL (0.8 mg mL^{-1})	68.4% (75 min)	-

Table S5. The internal quantum efficiency (IQE) of the samples

λ/nm		365	405	450	520
P/W		0.214	0.264	0.292	0.252
TCN-1	j_{ph}/mA cm^{-2}	7.50E-04	7.12E-04	7.93E-05	1.13E-05
	A	0.96	0.81	0.18	0.16
	IQE/%	41.99	30.65	6.89	1.09
TCN-2.5	j_{ph}/mA cm^{-2}	7.16E-04	6.57E-04	9.00E-05	1.27E-05
	A	0.98	0.87	0.20	0.15
	IQE/%	39.89	27.65	7.31	1.27
TCN-5	j_{ph}/mA cm^{-2}	9.76E-04	1.08E-03	1.42E-04	1.33E-05
	A	1.01	0.88	0.20	0.15
	IQE/%	53.87	45.23	11.40	1.34
TCN-8	j_{ph}/mA cm^{-2}	9.13E-04	8.79E-04	1.18E-04	1.13E-05
	A	1.02	0.89	0.22	0.16
	IQE/%	50.25	36.71	8.71	1.08
TCN-10	j_{ph}/mA cm^{-2}	7.70E-04	8.17E-04	1.23E-04	1.20E-05
	A	1.01	0.89	0.20	0.14
	IQE/%	42.54	34.18	9.82	1.31

References

1. J. Song and M. Z. Bazant, *Phys. Rev. Lett.*, 2018, **120**, 116001.
2. T. G. Nguyen, M. D. Nguyen, T. L. Do, V. T. Dang, T.-B. Nguyen and V. Hoang Huong, *Surfaces and Interfaces*, 2024, **54**, 105009.
3. X. Lin, Y. Ke, Y. Liu, X. Li, Z. Yu, D. Jiang and Y. Yuan, *International Journal of Hydrogen Energy*, 2024, **80**, 1234-1242.
4. B. Yang, J. Zhao, Y. Xiong, C. Li, M. Zhang, R. D. Rodriguez and X. Jia, *Chemical Engineering Journal*, 2024, **498**, 155117.
5. S. Li, Y. Yang, S. Wan, R. Wang, M. Yu, F. Song and Q. Zhong, *J. Colloid Interface Sci.*, 2023, **651**, 726-733.
6. Y. Ma, F. Liu, Y. Liu, X. Lan, Y. Zhu, J. Shi, W. Jiang, G. Wang and S. H. Park, *Chemical Engineering Journal*, 2021, **414**, 128802.
7. F. Guo, Z. Chen, Y. Shi, L. Cao, X. Cheng, W. Shi, L. Chen and X. Lin, *Renewable Energy*, 2022, **188**, 1-10.
8. X. Bai, M. Li, J. Li, X. Rao, S. Zheng and Y. Zhang, *ACS Applied Nano Materials*, 2022, **5**, 691-701.
9. T. Wu, Q. He, Z. Liu, B. Shao, Q. Liang, Y. Pan, J. Huang, Z. Peng, Y. Liu, C. Zhao, X. Yuan, L. Tang and S. Gong, *Journal of Hazardous Materials*, 2022, **424**, 127177.
10. H.-X. Fang, H. Guo, C.-G. Niu, C. Liang, D.-W. Huang, N. Tang, H.-Y. Liu, Y.-Y. Yang and L. Li, *Chemical Engineering Journal*, 2020, **402**, 126185.
11. R. Zhao, J. Gao, S. Mei, Y. Wu, X. Wang, X. Zhai, J. Yang, C. Hao and J. Yan, *Nanotechnology*, 2017, **28**.
12. R. C. Pawar, S. Kang, J. H. Park, J.-h. Kim, S. Ahn and C. S. Lee, *Scientific Reports*, 2016, **6**, 31147.
13. J. Fu, B. Zhu, C. Jiang, B. Cheng, W. You and J. Yu, *Small*, 2017, **13**, 1603938.
14. M. Tahir, C. Cao, F. K. Butt, F. Idrees, N. Mahmood, Z. Ali, I. Aslam, M. Tanveer, M. Rizwan and T. Mahmood, *Journal of Materials Chemistry A*, 2013, **1**, 13949-13955.
15. S. Wang, C. Li, T. Wang, P. Zhang, A. Li and J. Gong, *Journal of Materials Chemistry A*, 2014, **2**, 2885-2890.
16. Y. Gong, J. Chen, D. Ma and J. Zhong, *J. Colloid Interface Sci.*, 2025, **682**, 446-459.
17. Y. Ke, Q. You, J. Ai, X. Yang, Q. Shang, Y. Liu, D. Wang and G. Liao, *Journal of Materials Science & Technology*, 2023, **152**, 37-49.
18. S. M. Ghoreishian, K. S. Ranjith, M. Ghasemi, B. Park, S.-K. Hwang, N. Irannejad, M. Norouzi, S. Y. Park, R. Behjatmanesh-Ardakani, S. M. Pourmortazavi, S. Mirsadeghi, Y.-K. Han and Y. S. Huh, *Chem. Eng. J.*, 2023, **452**, 139435.
19. Y. Li, W. Wei, Z. Guo, L. Zou, M. Li, L. Ai and A. Wei, *Sep. Purif. Technol.*, 2022, **299**, 121730.

20. M. Wang, Y. Zeng, G. Dong and C. Wang, *Chin. J. Catal.*, 2020, **41**, 1498-1510.
21. V. Hasija, P. Singh, S. Thakur, K. Stando, V.-H. Nguyen, Q. V. Le, S. M. Alshehri, T. Ahamad, K. C. W. Wu and P. Raizada, *Appl. Mater. Today*, 2022, **29**, 101676.
22. D. Das, B. K. Das, R. Sarkar, S. Mukherjee and K. K. Chattopadhyay, *Environ. Res.*, 2023, **221**, 115263.